SUPPLEMENTAL MATERIALS

ASCE *Journal of Infrastructure Systems*

Framing the Use of Climate Model Projections in Infrastructure Engineering: Practices, Uncertainties, and Recommendations

Yuchuan Lai, Tania Lopez-Cantu, David A. Dzombak, and Constantine Samaras

DOI: 10.1061/(ASCE)IS.1943-555X.0000685

www.ascelibrary.org

Section S1. Statistical Forecasts and Projections of Regional Temperature and Precipitation for Engineering Applications

While use of climate model projections is a more common approach of facilitating engineering applications with future climate conditions, an alternative to climate models is to use statistical forecasting techniques on the basis of historical regional climate observations. For example, Cheng et al. (2014) provided a method of integrating non-stationarity into extreme value analysis to forecast temperature and precipitation extremes. Lai and Dzombak (2020) utilized long-term historical trends at different U.S. cities to provide near-term forecasts in various climate variables. As indicated in Figure 1 of the main text, the approach of using statistical forecasting provides a different option for applying climate model projections.

Use of historical observations and statistical forecasting provides an efficient and interpretable approach but can also be subject to limitations. Previous studies such as Krakauer and Fekete (2014) have showed that, extrapolation of historical trends can provide reliable local precipitation information for up to 25 years in the future. In addition, statistical forecasting with historical data can be "advantageous" to practitioners as Hyman et al. (2014) has argued. An integrated technique that combines statistical forecasting with the global climate model projections was developed in Lai and Dzombak (2021), serving as an additional alternative. However, use of historical observations and statistical forecasting techniques depends on the availability and quality of regional historical climate data. Due to the scope of this work, evaluation of statistical forecasting methods in engineering applications were not further analyzed.

Section S2. Integrating Climate Projections in Engineering Applications

As discussed in the main text, a wide range of techniques have been applied for integrating climate projections among engineering applications, leading to different climate variable formats required. The required climate variable formats are indicated in part A of Figure 1 of the main text. Overall, provided with time series of future climate variables, methods that use these time series for climate projections can be generally categorized into two main types regarding their use in engineering applications: using the time series as a direct input for engineering process models or further processing the projections to obtain climatic variable values (instead of the original time series).

The first type refers to the applications that feed future time series of climate variables into process models (or impact models) to analyze impacts of climate change in the system, e.g., Mechanistic–Empirical Pavement Design Guide model (Meagher et al. 2012), Variable Infiltration Capacity model (Van Vliet et al. 2016), and Infrastructure Planning Support System (Chinowsky et al. 2019). The integration of GCMs and process models was also referred as "chain-of-models" approach (NASEM 2018).

On the other hand, time series of climate variables may be further utilized to produce derived series or variables such as annual maxima (Tryhorn and Degaetano 2011), annual partial duration (DeGaetano and Zarrow 2011), annual degree days (Chaturvedi et al. 2013), pavement temperatures (Underwood et al. 2017). These derived variables are utilized to estimate "climatic design values" (Auld et al. 2010); and this variable format is referred to as climatic design values (compared to the use of time series in the previous approach).

Consequently, the types of methods to incorporate climate model projections in engineering applications can limit the applicable climate datasets or the available decisions, similar to the requirements on the temporal and spatial resolutions of climate projections as presented in part A of Figure 1 of the main text. For example, when the chain-of-model approach is applied and daily temperature and precipitation are required, quantile mapping may be the more appropriate post-processing techniques as it can consider the different intensities and modify the distributions of daily temperature and precipitation projections (Maraun et al. 2010).

At the same time, when climatic design values are derived from the time series of climate model projections, a change factor method can be applied to modify these estimated climatic design values. For example, during the two performed case studies, the change factor technique was utilized in this way to adjust the estimates of pavement maximum design temperatures in Los Angeles (LA) and the 1-day precipitation amount with 5-year return period in New York City (NYC) as a post-processing adjustment.

Information about the use of the two methods of integrating climate model projections and number of GCMs used in the review of 50 engineering applications reported in the literature is provided in Table S1, as a supplement to the information provided in the Table 1 of the main text. Identification of the use of the two methods in these previous studies was conducted based on our assessment of the information provided in the studies, and such information was not included in Figure 2 of the main text because many studies did not explicitly describe the formats of climate variables used and the results in Table S1 are thus subject to limitations.

Table S1. Additional information on the identified engineering studies in which climate model projections of future temperature and (or) precipitation were used

Sectors	IDs	Topics	Studies	Implementation methods[a]	Number of GCMs used[b]	Notes[c]
Buildings and other structures	1	Building energy with roof design	Hosseini et al. (2018)	DCV	HadCM3	The "morphing" method by Jentsch (2013) t modify weather files
	2	Building energy use	Reyna and Chester (2017)	DCV	10	Use of the "morphing" method
	3	Building energy use	Shen (2017)	DCV	HadCM3	Use of the "morphing" method
	4	Carbonation of concrete structures	Talukdar and Banthia (2016)	COM	CanESM2	Projections of CO2 concentrations were alsc used to study the carbonation in concrete
	5	Corrosion of steel structures	Nguyen et al. (2013)	DCV	9	The GCM projections were adjusted with pattern scaling by OzClim; relative humidity and wind speed were also used
	6	Energy and building performance	Jentsch et al. (2013)	DCV	HadCM3	Modify existing weather files using climate model projections
	7	Landslide	Peres and Cancelliere (2018)	COM	3	The GCM projections were used to perturb the parameters of a rainfall generator
	8	Urban heat island effect	Zhang and Ayyub (2018)	DCV	10	ARRM method was used to downscale and bias correct GCM projections
	9	Urban planning	Carter et al. (2015)	DCV	12 (UKCP09)	Climate data are provided by WGs (with RCM-modified parameters); including other climate change impacts assessed
Cold Regions	10	Alaska infrastructures	Melvin et al. (2017)	COM; DCV	5	Alaska specific Sta.Dwn-GCM (monthly resolution); temporal disaggregation to daily data
	11	Design ice loads	Jeong et al. (2019)	COM	CanESM2	Calculation of ice accretion is based on freezing precipitation amount
	12	Permafrost	Hjort et al. (2018)	DCV	15	WorldClim data were used (with statistical downscaling and bias correction)
	13	Rain-on-snow flood	Musselman et al. (2018)	DCV	19	The GCM projections were used to perturb the parameters of WRF model
Energy	14	Electricity distribution with wood poles	Merschman et al. (2020)	DCV	All GCMs in BCSD	Impacts from hurricanes were also considere
	15	Electricity systems with temperature	Sathaye et al. (2013)	DCV	3	
	16	Electricity transmission capacity	Bartos et al. (2016)	COM	11	Thermal model was calibrated with historica observations
	17	Electric power supply	Bartos and Chester (2015)	COM	2	
	18	Peak electricity demand	Auffhammer et al. (2017)	COM	All GCMs in MACA (assumed)	A statistical model was used to calculate energy load with daily weather data; unclear temporal resolution of MACA (assumed to l monthly)
	19	Peak electricity demand	Burillo et al. (2019)	COM	CCSM4	Dynamical downscaling with WRF model
	20	Power generation systems	Van Vliet et al. (2016)	COM	5	
	21	Water stress for power production	Ganguli et al. (2017)	DCV	45	Water availability is based on GCM while stream temperature was based on BCSD (with calibration on observed stream temperature)
Transportation	22	Aircraft takeoff performance	Coffel et al. (2017)	DCV	27	Temporal disaggregation to hourly data
	23	Bridges with floods	Wright et al. (2012)	DCV	4	Peak flows were estimated with 100-year peak precipitation amount; change of peak flows with the historical level was calculate
	24	Culvert with wildfire debris	FHWA (2017)	DCV	11	Sta.Dwn-GCM (unclear which one); 24-hou precipitation amounts were assessed
	25	Pavement	Underwood et al. (2017)	DCV	19	Possible alternative: AASHTO
	26	Pavement	FHWA (2016a; b)	DCV	11	Sta.Dwn-GCM (unclear which one); unclear whether further bias correction method was used
	27	Pavement	Mallick et al. (2014)	COM	GFDL	Including impacts from temperature and precipitation increase, sea level rise, and hurricanes
	28	Pavement	Meagher et al. (2012)	COM	3	Temporal disaggregation from 3-hr to 1-hr; include temp, prcp, wind spd, perc sunshine humidity as input
	29	Rail networks	Chinowsky et al. (2019)	COM	5	Infrastructure Planning Support System was used to incorporate climate projections and calculate different variables
	30	Rail networks	Palin et al. (2013)	DCV	HadCM3	Rail networks in the U.K.

	31	Roadway network with flash floods	Kermanshah et al. (2017)	DCV	CCSM4	Daily precipitation was used to calculate 5% thresholds
Urban Water Systems	32	Detention basin	Moglen and Rios Vidal (2014)	DCV	2	NOAA Atlas 14 were used as the historical rainfall amounts
	33	Water distribution systems	Bondank et al. (2018)	DCV	Ensemble; unclear how many	Sta.Dwn-GCM (unclear which one)
	34	Water utilities	Vogel et al. (2015) – NYCDEP	COM	15-20	
	35	Water utilities	Vogel et al. ((2015) - PWB	COM	20	Including other climate variables
	36	Water utilities	Vogel et al. 2015) - SPU	COM	20	Temporal disaggregation to hourly data
	37	Water utilities	Vogel et al. (2015) - TBW	COM	NA	Decided Dyn.Dwn-GCM as a supplement; various Dwn. techniques compared
	38	Sewer overflow	Fischbach et al. (2017)	COM	2	
	39	Stormwater	Cook et al. (2017)	DCV	6	Temporal disaggregation to hourly data
	40	Stormwater	Zahmatkesh et al. (2015)	COM	All GCMs in BCCA	Daily precipitation was used to calculate 5% thresholds
	41	Stormwater	Rosenberg et al. (2010)	COM	1 model for each scenario	Hourly precipitation projections were fitted hydrologic model to estimate streamflow
Water Resources	42	Eutrophication with precipitation	Sinha et al. (2017)	COM	16	Separate datasets used for the U.S. and the world; temperature data was also utilized
	43	Freshwater algal blooms	Chapra et al. (2017)	COM	5	Including other climate variables; not clear whether further bias correction method was used
	44	Ground water resources	Shrestha et al. (2016)	COM	5	The GCM projecitons were adjusted with pattern scaling
	45	Water quality	Gelda et al. (2019)	COM	20	Temporal disaggregation to hourly data; including other climate variables; water quality models were not yet utilized
	46	Water quality	Boehlert et al. (2015)	COM	IGSM-CAM	
	47	Water quality	Chang et al. (2015)	COM	24	
	48	Water quality and quantity	Alamdari et al. (2017)	COM	CCSM	Utilized historical data to calibrate SWMM model
	49	Water resource infrastructures	Drum et al. (2017)	COM	9	Sta.Dwn-GCM (unclear which one)
	50	Streamflow	Robinson and Herman (2019)	COM	All BCSD	Verify with historical streamflow data

[a] COM: chain-of-model approach; DCV: derived climatic values

[b] When one GCM was used, the name of the GCM is specified

[c] Sta.Down: Statistically downscaled projections; Dyn.Down: Dynamically downscaled projections

Section S3. GCMs and downscaling methods

Additional descriptions and background information of GCMs and downscaling approaches are provided in this section, as a supplement to the discussions provided in the main text.

S3-1. GCMs

GCMs resolve different physical processes such as coupled interactions between oceans and land with the integration of future greenhouse gases concentration. Projections from GCMs can be acquired from the World Climate Research Programme's Coupled Model Intercomparison Project (CMIP), currently at phase 6 (Eyring et al. 2016a), while the downscaled projection products commonly used in engineering applications belong to phase 5 (Taylor et al. 2012). GCMs from CMIP5 can provide historical simulations as early as 1850 and future projections up to 2300 (Taylor et al. 2012) and therefore the GCM projections generally satisfy all required infrastructure design lives.

It is important to note that GCMs are subject to different model designs and assumptions (such as different climate sensitivity, response time of global temperature increase, and ocean heat uptake (Taylor et al. 2012)) and the selection and inclusion of different GCMs can be a major source of uncertainty during engineering practices. The individual projections or the model bias values of GCMs depend on the their underlying assumptions or limitations in solving physical processes, e.g., a warm bias from several GCMs in upwelling zones at west coast of continents including west coast of the U.S. (Eyring et al. 2019). A careful selection of GCMs can potentially reduce errors for a studied region (Maraun et al. 2017), however, such process was seldom conducted for engineering applications. A more commonly employed approach is to utilize a number of

different GCMs and create an ensemble of projections in engineering applications, such as in Cook et al. (2017).

Spatial resolution should be determined for the use of GCM projections; and downscaling techniques are required if raw GCM projections do not satisfy the requirement in spatial resolutions. Depending on individual models, GCMs are limited in the spatial resolutions when solving global climate processes and the resolutions are generally about 100 km (Pierce et al. 2014). Consequently, the low resolutions of GCMs can limit the capability of representing regional climate for engineering applications (Jack and Katragkou 2019) and downscaled GCM projections will be preferred for these applications. Downscaling methods are further discussed in the Section C-2.

Additionally, for a particular engineering application, one or several future climate change scenarios should be selected, representing the uncertainty in future greenhouse gas concentrations (Moss et al. 2010) and, in the more recently developed CMIP6, with the additional consideration of socioeconomic scenarios (O'Neill et al. 2017) . In CMIP5, different representative concentration pathways (RCPs) refer to the uncertainty in determining future climate conditions inherited from different possible human response to the changing climate (Moss et al. 2010). A high concentration scenario should be considered if the impact assessment is decided to be more conservative.

S3-2. Downscaling

Because GCMs are in low spatial resolution (~100km) and often projections with higher resolutions are needed to represent regional climate, downscaled GCM projections – with the integration of GCM projections and downscaling techniques – can be obtained to facilitate

engineering applications. Downscaling techniques can be generally categorized into two approaches, i.e., dynamical and statistical downscaling methods.

To provide finer-resolution forecasts, RCMs were utilized to resolve regional-scale atmospheric-land-ocean coupled physical processes using GCM projections as boundary conditions (Hall 2014). Because the physical processes that govern the magnitude and variations of climate variables are explicitly resolved in RCMs, results from dynamical downscaling are physically consistent. Examples of dynamical downscaled projections include the North America - Coordinated Regional Climate Downscaling Experiment (NA-CORDEX; Giorgi and Gutowski 2015) of CMIP5 and North American Regional Climate Change Assessment Program (NARCCAP; Mearns et al. 2009) of CMIP3.

Because the use of an RCM can explicitly resolve climate variables in daily or sub-daily time-step, dynamically downscaled projections with sub-daily resolutions can be provided (Cook et al. 2017). Engineering applications that require sub-daily projections (e.g., to assess intensity of precipitation extremes) are consequently limited to the dynamically downscaled projection products if temporal disaggregation is not employed, as also discussed in the main text.

On the other hand, instead of using RCMs to resolve regional physical processes, a second category of downscaled projections are directly produced based on statistical relationship between fine-resolution historical observations and GCM projections. These statistical downscaling procedures provide the fine-resolution regional projections by assuming projected larger weather phenomenon in GCMs is statistically correlated with finer observed regional/local weather phenomena (Maraun et al. 2010). Linear and non-linear regression models and analog methods are some examples of statistical downscaling techniques. Examples of downscaled GCM datasets (some were specifically developed for the U.S. or North America) include, bias

corrected constructed analogs (BCCA; Brekke et al. 2013), localized constructed analogs (LOCA; Pierce et al. 2014), and multivariate adaptive constructed analogs (MACA; Abatzoglou and Brown 2012).

As exhibited in Figure 2 of the main text, statistical downscaled GCM projections are the more commonly utilized climate model projections in the 50 previously reported engineering applications examined in this work. However, the particular types of statistical downscaled GCM projection products vary among different studies and the reasons why a particular type was used were often not discussed. Studies like Kilgore et al. (2019) have recommended and utilized LOCA in hydrological designs because the LOCA products were specifically resolved in the shapes of daily forecast distributions and belong to the more recent CMIP5 instead of the previous phase CMIP3.

Section S4. Post-processing Techniques

Further descriptions of post-processing techniques and methodology of applying these techniques are provided in this section, in addition to the discussions provided in the main text.

The post-processing techniques include methods to increase the level of agreement between model projections and historical observations. This is because that discrepancy or model bias can still exist between model grid-level simulations and historical observations (especially when compared to station-level observations), although finer-resolution downscaled projections may be already obtained. Note that this type of post-processing technique also has been referred to as "downscaling" in some previous studies such as in Switzman et al. (2017), however, such a term was not adopted in this work to avoid confusion with downscaled projection products and because these post-processing techniques require an action of processing the projection results for engineers. Because of the discrepancy between model projections and historical observations, these further processing techniques are often necessary to transfer the gridded model projections to match the historical observations in station (or point) level, as studies like Mannshardt-Shamseldin et al. (2012) suggested. Additionally, because dynamical downscaling techniques rely on RCMs to resolve physical processes and is limited by computational power, the highest spatial resolutions of dynamical downscaled GCM projections over the U.S. are typically at 0.22º (about 25 km) in NA-CORDEX (Mearns et al. 2017), and thus post-processing techniques may be needed to transfer to station-level projections. Both change factor and quantile mapping can be used for increasing the alignment of projections with observations.

The post-processing techniques can also be applied for temporal disaggregation to facilitate the use of climate model projections in finer temporal resolutions. Given that required temporal

resolution can be a constraint in selecting climate model projections, both change factor or quantile mapping can be used as temporal disaggregation techniques to post-process and obtain projections at finer temporal resolutions. Historical observations at desired temporal resolutions are required, however.

Furthermore, some engineering applications have specific requirements involving the use of weather files produced by weather generators; and GCM projections are often used to modify the parameters of weather generators during post-processing. Weather generators are statistical simulation models that can produce sequences of weather variables based on parameterization and correlation of different variables (Wilks and Wilby 1999). As further discussed in Section D-3 of Supplemental Material, climate model projections are post-processed in this case to consider effect of future climate change on the output of weather generators (referred as GCM-modified weather files in this work).

Depending on the specific engineering applications, it is important to note that a particular post-processing technique can be applied differently and can be applied with different purposes. For example, a change factor technique can be applied to adjust a whole continuous time series of climate variables prior to the utilization of such a time series or to modify derived climate variables (estimated from unmodified projections) as a final adjustment. At the same time, techniques like change factor can be used with the purposes of correcting bias as well as performing temporal disaggregation.

S4-1. Change factor

Change factor (or delta) method is a common post-processing technique used in engineering applications. During the post-processing, historical observed climate variables are added (for

temperature) or multiplied (for precipitation) with a ratio estimated between historical and future simulations from a single GCM or an ensemble of GCMs (Maraun 2016). The change factor approach is based on the following:

$$y_{modeled\ future;\ modified} = \frac{y_{hist,observed}}{y_{hist,modeled}} \times y_{future,modeled} = \frac{y_{future,modeled}}{y_{hist,modeled}} \times y_{hist,observed}$$
$$= CF \times y_{hist,observed} \quad \text{(S1)}$$

where $y_{\text{modeled future; modified}}$ is the change-factor-modified future climate variables in the projected period, $y_{\text{hist, observed}}$ is the historical observed climate variables, $y_{\text{hist, modeled}}$ is the historical simulated climate variables from climate models, and $y_{\text{future, modeled}}$ is the future simulated climate variables from climate models.

A similar approach to the change factor method is the direct method, in which a ratio between historical observations and modeled historical simulations is estimated to adjust GCM future simulations (Maraun 2016).

Change factor method can be applied to transfer grid-level model projections to station-level or used as a temporal disaggregation technique, as mentioned previously. For example, stormwater runoff assessment is commonly employed with change factor to adjust rainfall volume and intensity in previous studies, as presented in Table 1 and Figure 2 of the main text. On the other hand, change factor were also used to produce hourly precipitation amount, e.g., in Zahmatkesh et al. (2015).

S4-2. Quantile mapping

In contrast to adjusting the mean or percentiles with the ratios in the change factor method, quantile mapping is a more flexible post-processing technique by adjusting the distributions of

climate model projections. In quantile mapping, a reference period is used to establish a relationship (or transfer function; Maraun 2016) between the distributions of historical observation and the distributions of GCM historical simulations. This transfer function is then applied to GCM future simulations to reduce model bias or to produce station-level projections. Consequently, the use of transfer functions in a quantile mapping approach is similar to the calculation and applying of ratios in the direct method mentioned previously.

Quantile mapping techniques have been applied in previous studies and for different purposes. For example, Kuo et al. (2014) utilized a quantile mapping method on dynamical downscaled GCM projections to reduce model bias and assessed future extreme precipitation events at Alberta, Canada. Studies like Mannshardt-Shamseldin et al. (2012) have used quantile mapping to modify the distributions of downscaled GCM projections to match the station-level observations. Moreover, quantile mapping techniques have also been utilized to tailor the model projections and match the required temporal resolutions, such as in Coffel et al. (2017) and Meagher et al. (2012), as presented in Table 1 and Figure 2 of the main text.

S4-3. GCM-modified weather files

Weather generators are commonly used to provide weather files for engineering applications such as in building energy use estimation (Shen 2017). The GCM-modified weather files can be used to consider future climate change in these engineering practices. The GCM-modified weather files are obtained by utilizing climate model projections to modify or "perturb" (Maraun et al. 2010) different parameters in weather generators, e.g., change factors can be calculated from climate model projections to perturb the parameters. While the GCM-modified weather generators are a traditional approach, more advanced weather generators like full-field weather

generators also exist and have shown more potential (Maraun et al. 2010). Note that in the case of GCM-modified weather generators, weather generators provide the source of climate datasets for engineering applications while climate model projections are only used (i.e., post-processed) to modify the parameters of weather generators. Because the nature of some engineering practices requires the use of weather files, the GCM-modified weather files were more often utilized in these practices as presented in Table 1 and Figure 2 in the main text.

S4-4. Other techniques

Several other techniques can also be used to post-process climate data to facilitate engineering applications, for the purposes of bias-correcting model projections or providing projections in a desired format. For example, methods like linear extrapolation can be used to perform temporal disaggregation for temperature (Coffel et al. 2017). An approach of obtaining weights for different downscaled GCM projections and using a "probabilistic simple climate model" (Rasmussen et al. 2016) to produce probabilistic projections has been utilized to evaluate future economic damages caused by climate change in the U.S. (Houser et al. 2017). Regression models, e.g., in Mannshardt-Shamseldin et al. (2012), can be used to establish the transfer function between GCM simulations and historical observations to improve model bias. Similar to the use of weather generators, these approaches require more steps of post-processing. Applications of these alternative approaches in engineered systems and evaluation of the uncertainty from these techniques were not further assessed in this work.

Section S5. Specifications for Two Case Studies

Detailed descriptions of the calculation processes for the case studies of the high-temperature PG grade for asphalt binder during pavement design in LA and the stormwater drainage pipe diameter for a design relevant to a 1-hour, 5-year-return storm in NYC are provided in this section, as supplements to the discussions provided in the main text.

S5-1. Case study of selecting high-temperature PG grade for pavement design in LA

Estimates of maximum pavement design temperature and the subsequent selection of high-temperature PG grade for asphalt concrete pavement design in LA were used as a case study of incorporating temperature projections in engineering applications. While the PG grade also requires an estimate of minimum design temperature (and subsequent selection of low-temperature grade), the maximum design temperature was assessed in this study because the maximum pavement design temperature is expected to be more substantially affected by climate change impact – a higher design temperature will lead to a higher asphalt binder requirement. Following the PG method, the maximum pavement design temperature can be calculated as (TRB Superpave Committee 2005; Underwood et al. 2017):

$$T_{pav,high} = 0.9545\left(\left(T_{air,high} + z \times \sigma_{air,high}\right) - 0.00618Lat^2 + 0.2289Lat + 42.2\right) - 17.78 \quad (S2)$$

where $T_{air,high}$ and $\sigma_{air,high}$ are the average and standard deviation of annual warmest consecutive-seven-day T_{max} for a particular period (moving 30-year periods in this case), Lat is the latitude of the study location, and z is the z-score for normal distribution as a consideration for pavement reliability. A 98% reliability (with $z = 2.055$) was used for the analyses in this study. The annual consecutive-seven-day T_{max} is estimated as an average of T_{max} for the seven consecutive days.

The calculated values of pavement maximum temperature (at 98% reliability) can be then used to select the corresponding high-temperature PG grade. Further adjustments and offset values can be included or added to the calculated pavement maximum temperature to consider the additional damages from traffic and consider the pavement depths (FHWA 2016a), although such adjustments were not made in this case study. For the high-temperature PG grade, the commonly available increments are: 46, 52, 58, 64, 70, 76, and 82 ºC (Underwood et al. 2017), which were used for determining the selected high-temperature PG grade in in this case. Based on the estimated maximum pavement design temperature, the first increments higher than the pavement maximum temperature were selected, e.g., if the maximum pavement design temperature is estimated at 65 ºC, a 70-ºC grade is selected.

S5-2. Case study of selecting pipe diameter for stormwater drainage design in NYC

The case study of stormwater drainage design in NYC was based on the estimates of 1-day precipitation amount with 5-year return period and subsequent selection of pipe diameter for a design of 1-hour, 5-year-return storm. While precipitation amounts with other return periods can also be calculated, this study focused on the effect of different decisions on the estimates of climatic design values and thus the amount with 5-year return period (which has a relatively higher recurrence rate) was calculated. Similarly, the estimation of pipe diameters for other storms (e.g., 30-min, 5-year return or 2-hour, 5-year-return storm) can be conducted. Here, the design was based on the 1-hour, 5-year-return storm using a similar calculation for a 1-hour storm as in Cook et al. (2020), following the same assumptions on the drainage area in Cook et al. (2020).

The estimation of stormwater drainage pipe diameters requires three steps in this case: the estimation of the maximum 1-day precipitation amount with 5-year return period, the estimation

of peak runoff with respect to the 1-hour, 5-year-return storm, and the estimation of pipe diameter based on the peak runoff.

The 1-day precipitation amount with 5-year return period was estimated by fitting annual maximum 1-day precipitation from a particular period (moving 30-year periods in this case) with General Extreme Value (GEV) distributions using L-moment in this study. Given the fitted GEV distribution, the 5-year return period is calculated as the amount of precipitation with an annual 20% probability of exceedance. It is worth noting that the GEV fitting is subject to uncertainties including the uncertainty from the estimated GEV parameters. These uncertainties were not considered and were excluded from the analyses in this work as the main objective of this work was to assess the possible different outcomes or sensitivity of the results caused by the different decisions made during the application of climate model projections.

Similar to the approach used in Cook et al. (2020), the Rational method was used in this study to estimate the peak runoff from the 1-hour, 5-year storm:

$$Q_p = ciA \qquad (S3)$$

where Q_p is the peak runoff for the drainage area (cubic feet per second), c is the runoff coefficient (unitless) for the landscape of interest, i is the rainfall intensity (inches per hour), and A is the drainage area (acres).

As in Cook et al. (2020), a moderately urbanized neighborhood with a drainage area of 10 acres was assumed and assessed in this case study. For the moderately urbanized neighborhood, the runoff coefficient c of 0.65 was used (Cook et al. 2020). To simplify the calculation, a relationship between the 60-min precipitation amount and 1-day precipitation amount (both with 5-year return period) in NOAA Atlas 14 (NOAA 2017) was used to obtain the projected 60-min

precipitation amount using the previous estimated 1-day precipitation amount (with 5-year return period). Note that the available precipitation amount (median estimates) in NOAA Atlas 14 is 1.61 inch for 60 minutes and 4.70 inch for 24 hours at the NYC Central Park station. The estimated 1-day precipitation amount from the previous step was adjusted to be the 24-hour amount (times 1.13) because the daily precipitation is reported for a fixed 24-hour interval and can be less than the maximum 24-hour precipitation amount. The adjustment ratio 1.13 was based on the same value used in NOAA atlas 14 (DeGaetano and Zarrow 2011). Similarly, the 60-min precipitation amount was used as the precipitation intensity *i* for the design corresponding to a 1-hour storm.

After the peak runoff is estimated, the pipe diameter can then be calculated using the Manning's equation (Cook et al. 2020):

$$Dr = \left(\frac{nQ_p}{0.31k_n\sqrt{S_0}}\right)^{\frac{3}{8}} \quad (S4)$$

where *Dr* is the pipe diameter, *n* is the roughness coefficient, S_0 is the channel slope, and $k_n$is a coefficient of the velocity versus slope relationship.

Following the same assumptions made for the case study in Cook et al. (2020), the roughness coefficient was assumed to be 0.013 for ordinary concrete lining, k_n equals 1, and S_0 equals 0.005 (as 0.5%).

Similar to the selection of high-temperature PG grade in the previous case study, the stormwater drainage pipe size can be determined based on the available increments for the pipe diameters. The available increments around the estimated pipe diameters are: 18, 21, 24, 27, 30, 36, and 42 inches (corresponding to 450, 525, 600, 675, 750, 900, and 1050 mm; Cook et al. 2020), and in this case, the first increments larger than the estimated pipe diameters *Dr* were selected.

S5-3. Post-processing and the calculation of 30-year moving estimates

For the two case studies, post-processing techniques were applied with the projection results obtained from different downscaled projection products, GCMs, and climate change scenarios (using both climate projections and historical observations) to estimate the values of maximum pavement temperature with 98% reliability in LA and maximum 1-day precipitation amount with 5-year return period in NYC. The climate model projections were acquired at the grid locations nearest to two local weather stations for the two cities (Los Angeles Downtown/USC station, GHCN ID: USW00093134; New York City Central Park station, GHCN ID: USW00094728). These two downtown weather stations provide continuous long-term historical records (starting from 1878 for Los Angeles and 1869 for New York City) for the two cities (more information can be found at National Weather Service website such as https://www.weather.gov/okx/CentralParkHistorical or Lai and Dzombak (2019)). The historical observations for the two weather stations were then used to evaluate and post-process the climate model projections.

The two post-processing techniques were applied in different ways to obtain the design values for the case studies. As discussed in the main text and in the previous section, the change factor approach modifies the results of the two estimated design values (i.e., the maximum pavement temperature with 98% reliability and the maximum 1-day precipitation amount with 5-year return period) based on the estimates from the historical observations and GCM historical simulations. The quantile mapping technique (a non-parametric method, which matches the empirical cumulative distributions with 20 quantiles, was used in this study) modifies the daily temperature and precipitation projections prior to the estimation of the two design values. Both post-processing techniques require a particular reference period. Two different 30-year periods

(1961-1990 and 1991-2020) were used as the historical reference periods for the case studies, with the results presented in Figures S1 (further discussed) and Figure 6 in the main text.

Furthermore, it is important to note that moving 30-year estimates were calculated and are presented for the two case studies, similar to the moving 30-year averages of the annual average temperature and precipitation presented in Figures 3 and 4 of the main text. The use of 30-year moving estimates is to facilitate the calculation of average and standard deviation of annual warmest consecutive-seven-day T_{max} in Eq.(S2) and to reduce the effect of annual variations presented in the temperature and precipitation series (similar to the effect from using a 30-year moving average filter). The process of applying moving 30-year estimate is (with the pavement design temperature estimates as an example): for each year in the series, annual maximum consecutive 7-day T_{max} of this year and 29 years prior were calculated; the calculated maximum consecutive 7-day T_{max} during this 30-year period was used to estimate $T_{air,high}$ and $\sigma_{air,high}$; and then the maximum design temperature was calculated using Eq.(S2) given the estimated $T_{air,high}$ and $\sigma_{air,high}$. For the graphs of 30-year moving estimates (or the 30-year moving averages) presented in this study (such as part (b13) of Figure 4 of the main text), the 30-year moving estimates are presented at the last years of the 30-year periods in the time series. For example, the maximum design temperature for 1975 exhibited in part (b13) of Figure 4 in the main text shows the results based on the daily temperatures during 1946-1975.

S5-4. Additional results for the assessment of post-processing in the two case studies

As a supplement to the results of Figure 6 presented in the main text, additional analysis and comparison on the use of two post-processing techniques with different downscaled projection products were conducted and are presented in this section. Specifically, the results of the two

case studies when different downscaled projection products from one GCM (CanESM2) with post-processing are presented in Figure S1. To provide more detailed evaluation of the two post-processing techniques (the change factor and quantile mapping methods), some additional findings on the results of Figure 6 in the main text (i.e., the LOCA downscaled results from 32 GCMs with post-processing) are provided in this section as well.

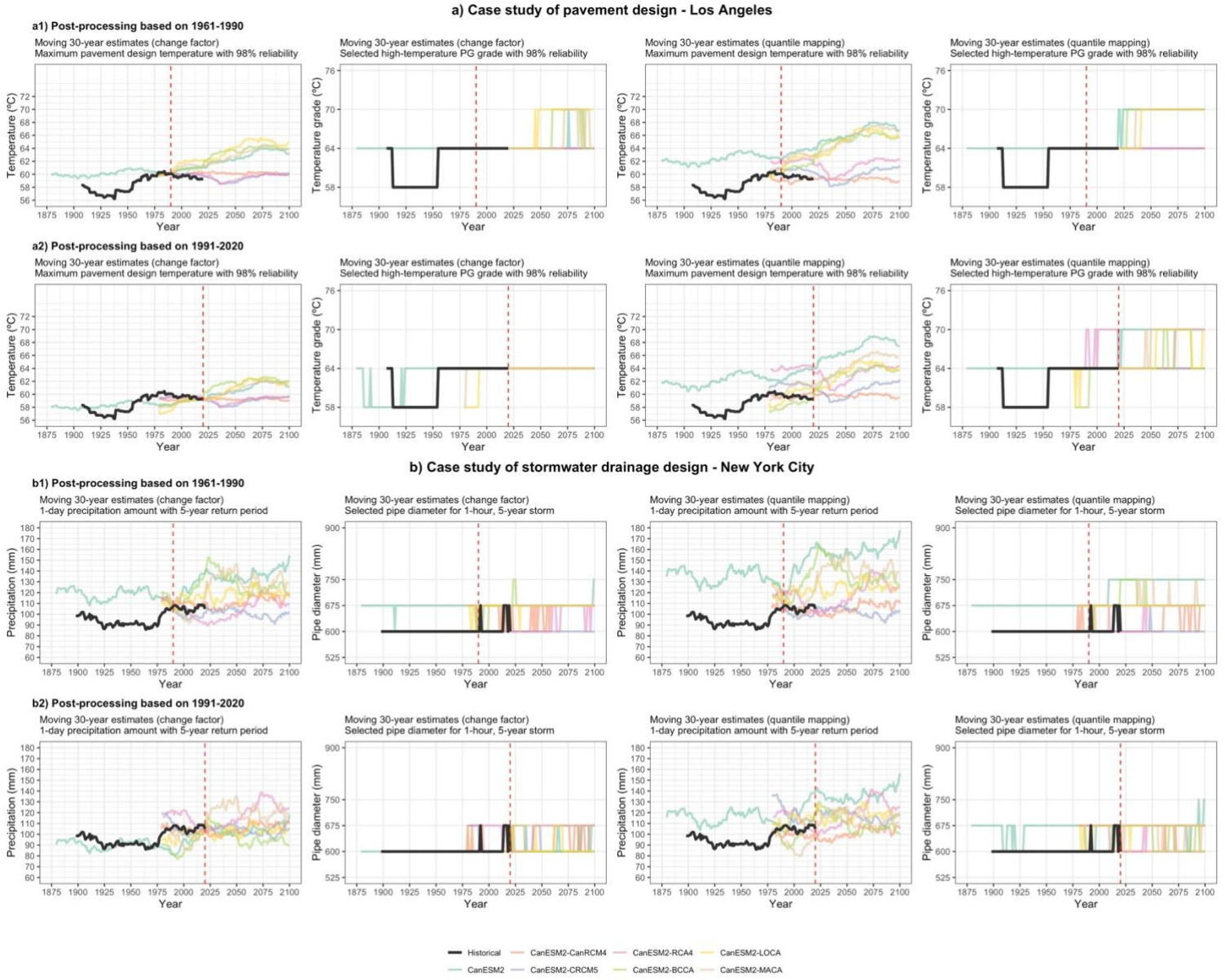

Figure S1. Assessing the use of post-processing techniques for different downscaled projection products in the two case studies. The first two columns present the results when the change factor method is used while the right two columns present the results when the quantile mapping method is used. Two reference periods were used (indicated as red vertical dashed lines): 1961-1990 period used in (a1) and (b1);

and 1991-2020 period used in (a2) and (b2). The moving 30-year estimates are presented for the time series. For the results of high-temperature PG grade and pipe diameter, the horizontal lines indicate the selected increments with the moving 30-year estimates (y-axes present the available increments) while the vertical lines indicate the increases (or decreases) of the increments based on the historical observations and different projections.

Similar to Figure 6 in the main text, the results of Figure S1 suggest that the post-processing techniques can improve the projection results, although these techniques are also subject to some limitations. While the quantile mapping moderately improved the alignment with the design values estimated from historical observations according to Figure S1, the change factor method can shift the design value estimates from the projections to the observation level more substantially. Some limitations of the post-processing techniques are evident in Figure S1, including the variations of results with different post-processing techniques (Cook et al. 2020), the inflated underlying future trends (Maraun 2013), the sensitivity to the selection of a reference period (Hawkins and Sutton 2016), and reducing the "added-values" (Karmalkar 2018) from downscaling methods. Notably, the raw GCM projections directly obtained from CanESM2, which exhibit significant model bias in Figure 4 in the main text, are comparable to the downscaled projections after post-processing in Figure S1. With the use of post-processing techniques, the differences between raw and downscaled GCM projections (and likely the added-values from downscaling) were consequently reduced, especially for the change factor presented in Figure S1. Considering that both statistical downscaling and post-processing techniques modify the projections based on statistical methods and historical observations, one statistically downscaled projection product is likely sufficient when post-processing is applied, as also mentioned in the main text. Dynamically downscaled projections produced from RCMs may provide additional regional information but are relatively limited to the number of GCMs and scenarios compared to the LOCA or other statistically downscaled projections.

Further, as presented in Figure 6 of the main text, one downscaled projection product (the LOCA projections) was assessed with the post-processing in order to compare and evaluate the results with different scenarios and GCMs. Similar to the findings in Figure S1, post-processing can be

useful to improve the alignment of the projections with the observations but can also be challenging. In Figure 6 of the main text, both the projection uncertainty from different GCMs and projected future trends were modified after applying with post-processing especially for RCP8.5. Compared to the results with no post-processing in Figure 5 of the main text, the uncertainty from different GCMs increased in Figure 6 of the main text especially for the precipitation-related case study in NYC. The selected high-temperature PG grades and pipe diameters generally are among the three increments, although the particular years for the increases of increment needed vary largely, suggesting large uncertainty in the projections. If different sources of uncertainties can be numerically combined (i.e., a sum of uncertainties from different GCMs, downscaling, future scenarios, and post-processing techniques as presented in Figures 6 of the main text and Figure S1), the uncertainty levels can be greater.

On the other hand, for these two case studies, the increase of one or two increments (depending on the historical baseline) will likely be sufficient to withstand the projected future changes of temperature and precipitation up to 2100, although the projected years that require the increases of increment are subject to large uncertainty. Therefore, depending on engineering applications, an ensemble of GCM projections (avoiding individual model errors) to understand the necessary adaptation efforts needed is potentially of greater value than projections for a specific time period (which are subject to substantial uncertainty). In addition, other post-processing techniques that can better integrate the GCM projections with the historical observations are potentially needed.

Section S6. Future Development for Use of Climate Model Projections

Research is in progress to improve the understanding on applying climate model projections (specifically for a particular climate-variable-related assessment or for assessment using different downscaling methods and different GCMs) and new versions of GCMs and downscaling products are being released in a continuous manner. To facilitate and incorporate the new information or new products of climate model projections in future engineering applications, some of ongoing research and studies are discussed in this section. The future development or improvement can potentially reduce the different stages of uncertainties with respect to the decisions involved, while the general procedures of applying climate model projections in Figure 1 of the main text are expected to remain applicable with the new model projections or information.

The first potential future development for engineering applications is the new phase of GCM projections. As also discussed in the main text, commonly used downscaled GCM projection products in the identified 50 engineering applications generally belong to CMIP5. The new source/phase of GCMs (phase 6, CMIP6; Eyring et al. 2016) has been released (Eyring et al. 2016a; IPCC 2017). As analyzed in Figure 3 in the main text, some GCM results from CMIP6 are available as of March 2021. One important development is the establishment of a new set of future socioeconomic scenarios – with different pathways considering socioeconomic changes – shared socioeconomic pathways (SSP; O'Neill et al. 2017), compared to the representative concentration pathways (RCPs) of CMIP5. Following the new phase of GCM projections, the new downscaled projection products are expected to be developed in the coming years, and promise to facilitate engineering applications with more recent climate model projections. Some

comparisons of the GCM projections between CMIP5 and CMIP6 for the two case locations (Los Angeles and New York City) are provided in Figure 3 of the main text.

To address the uncertainty from different downscaling methods, research such as EU Validating and Integrating Downscaling Methods for Climate Change Research (VALUE) project (Jack and Katragkou 2019) is in progress and aims to fulfill the user needs of evaluating different downscaling methods. These studies can provide insight about which downscaling methods are more appropriate for which types of applications. According to the first-stage results from VALUE project (Maraun et al. 2018), different downscaling approaches have different relative characteristics and a careful evaluation or deep understanding of utilized downscaling techniques is important when applying to a particular application.

Research is in progress to improve the understanding on the performance of different GCMs and reduce the uncertainty from the ensemble of different GCMs (Eyring et al. 2019). Earth System Model Evaluation Tool (ESMValTool; Eyring et al. 2016a) and Coordinated set of Model Evaluation Capabilities (CMEC; USDOE 2019) are some examples of GCM comparison and evaluation projects. Results of such effort can provide more guidance on questions like which GCMs can provide more accurate projections for which climate variables. Techniques such as multi-model weighting (Cannon 2015) and "Emergent Constraints" (Eyring et al. 2019) can be used to select the best performed GCMs or reduce uncertainty bounds during climate change impact assessments. Efforts such as the NOAA Regional Integrated Sciences and Assessments (RISA) program (Briley et al. 2020) and a USGS initiative (Terando et al. 2020), as also discussed in the main text, will help to bridge the gaps and to provide useful information on the

use of climate model projections in practical applications, e.g., the production of the "Consumer Report style" GCM documents (Briley et al. 2020).

Providing improved regional climate change assessments especially for state and local levels has been widely discussed and progress is being made. Climate model projections have been increasingly used in state and local climate change assessment plans such as Austin TX (City of Austin 2018), Boston MA (City of Boston 2016), Indianapolis IN (City of Indianapolis 2019), and New York State (DeGaetano and Castellano 2017), as also described in the main text. Recent development such as "Science for Climate Action Network" (SCAN; Moss et al. 2019) has provided a non-federal platform for collaboration between different communities, especially in providing improved regional climate information and facilitating practitioners such as civil and environmental engineers. Discussions about improving regional climate projections for practical applications can also been found in a number of recent studies (e.g., Arnott et al. 2016; Bremer et al. 2019; Kirchhoff et al. 2019; Martel et al. 2021). Together with improvement in downscaled GCM projections, such efforts can further reduce the challenges for engineers to incorporate regional climate information in engineering practices.

References

Abatzoglou, J. T., and Brown, T. J. (2012). "A comparison of statistical downscaling methods suited for wildfire applications." *International Journal of Climatology*, 32(5), 772–780.

Alamdari, N., Sample, D. J., Steinberg, P., Ross, A. C., and Easton, Z. M. (2017). "Assessing the effects of climate change on water quantity and quality in an urban watershed using a calibrated stormwater model." *Water (Switzerland)*, 9(7).

Arnott, J. C., Moser, S. C., and Goodrich, K. A. (2016). "Evaluation that counts: A review of climate change adaptation indicators & metrics using lessons from effective evaluation and science-practice interaction." *Environmental Science and Policy*, Elsevier Ltd, 66, 383–392.

Auffhammer, M., Baylis, P., and Hausman, C. H. (2017). "Climate change is projected to have severe impacts on the frequency and intensity of peak electricity demand across the United States." *Proceedings of the National Academy of Sciences of the United States of America*, 114(8), 1886–1891.

Auld, H., Waller, J., Eng, S., Klaassen, J., Morris, R., et al. (2010). "The Changing Climate and National Building Codes and Standards." *Ninth Symposium on the Urban Environment*, American Meteorological Society.

Bartos, M., Chester, M., Johnson, N., Gorman, B., Eisenberg, D., et al. (2016). "Impacts of rising air temperatures on electric transmission ampacity and peak electricity load in the United States." *Environmental Research Letters*, IOP Publishing, 11(11).

Bartos, M. D., and Chester, M. V. (2015). "Impacts of climate change on electric power supply in the Western United States." *Nature Climate Change*, 5(8), 748–752.

Boehlert, B., Strzepek, K. M., Chapra, S. C., Fant, C., Gebretsadik, Y., et al. (2015). "Climate change impacts and greenhouse gas mitigation effects on US water quality." *Journal of Advances in Modeling Earth Systems*, Wiley Online Library, 7(3), 1326–1338.

Bondank, E. N., Chester, M. V., and Ruddell, B. L. (2018). "Water Distribution System Failure Risks with Increasing Temperatures." *Environmental Science and Technology*, research-article, American Chemical Society, 52(17), 9605–9614.

Brekke, L., Thrasher, B. L., Maurer, E. P., and Pruitt, T. (2013). "Downscaled CMIP3 and

CMIP5 climate projections: release of downscaled CMIP5 climate projections, comparison with preceding information, and summary of user needs." *US Department of the Interior, Bureau of Reclamation, Technical Service Center, Denver, Colorado, USA*.

Bremer, S., Wardekker, A., Dessai, S., Sobolowski, S., Slaattelid, R., et al. (2019). "Toward a multi-faceted conception of co-production of climate services." *Climate Services*, Elsevier, 13(February), 42–50.

Briley, L., Kelly, R., Blackmer, E. D., Troncoso, A. V., Rood, R. B., et al. (2020). "Increasing the usability of climate models through the use of consumer-report-style resources for decision-making." *Bulletin of the American Meteorological Society*, 101(10), E1709–E1717.

Burillo, D., Chester, M. V., Pincetl, S., Fournier, E. D., and Reyna, J. (2019). "Forecasting peak electricity demand for Los Angeles considering higher air temperatures due to climate change." *Applied Energy*, Elsevier, 236(July 2018), 1–9.

Cannon, A. J. (2015). "Selecting GCM scenarios that span the range of changes in a multimodel ensemble: Application to CMIP5 climate extremes indices." *Journal of Climate*, 28(3), 1260–1267.

Carter, J. G., Cavan, G., Connelly, A., Guy, S., Handley, J., et al. (2015). "Climate change and the city: Building capacity for urban adaptation." *Progress in Planning*, Elsevier Ltd, 95, 1–66.

Chang, C. H., Cai, L. Y., Lin, T. F., Chung, C. L., Van Der Linden, L., et al. (2015). "Assessment of the impacts of climate change on the water quality of a small deep reservoir in a humid-subtropical climatic region." *Water (Switzerland)*, 7(4), 1687–1711.

Chapra, S. C., Boehlert, B., Fant, C., Bierman, V. J., Henderson, J., et al. (2017). "Climate Change Impacts on Harmful Algal Blooms in U.S. Freshwaters: A Screening-Level Assessment." *Environmental Science and Technology*, 51(16), 8933–8943.

Chaturvedi, V., Kim, S., Smith, S. J., Clarke, L., Yuyu, Z., et al. (2013). "Model evaluation and hindcasting: An experiment with an integrated assessment model." *Energy*, Elsevier Ltd, 61, 479–490.

Cheng, L., AghaKouchak, A., Gilleland, E., and Katz, R. W. (2014). "Non-stationary extreme value analysis in a changing climate." *Climatic Change*, 127(2), 353–369.

Chinowsky, P., Helman, J., Gulati, S., Neumann, J., and Martinich, J. (2019). “Impacts of climate change on operation of the US rail network.” *Transport Policy*, Elsevier Ltd, 75(July 2017), 183–191.

City of Austin. (2018). *Climate Resilience Action Plan for City Assets and Operations*. City of Austin Office of Sustainability.

City of Boston. (2016). *Climate Ready Boston*. City of Boston.

City of Indianapolis. (2019). *Thrive Indianapolis*. City of Indianapolis Office of Sustainability.

Coffel, E. D., Thompson, T. R., and Horton, R. M. (2017). “The impacts of rising temperatures on aircraft takeoff performance.” *Climatic Change*, Springer, 144(2), 381–388.

Cook, L. M., Anderson, C. J., and Samaras, C. (2017). “Framework for incorporating downscaled climate output into existing engineering methods: Application to precipitation frequency curves.” *Journal of Infrastructure Systems*, 23(4), 1–28.

Cook, L. M., McGinnis, S., and Samaras, C. (2020). “The effect of modeling choices on updating intensity-duration-frequency curves and stormwater infrastructure designs for climate change.” *Climatic Change*, Springer, 1–20.

DeGaetano, A. T., and Castellano, C. M. (2017). “Future projections of extreme precipitation intensity-duration-frequency curves for climate adaptation planning in New York State.” *Climate Services*, The Authors, 5, 23–35.

DeGaetano, A., and Zarrow, D. (2011). *Extreme Precipitation in New York & New England. Technical Documentation & User Manual*. Ithaca, New York.

Drum, R. G., Noel, J., Kovatch, J., Yeghiazarian, L., Stone, H., et al. (2017). *Ohio River Basin - Formulating Climate Change Mitigation/Adaptation Strategies through Regional Collaboration with the ORB Alliance*. *Civil Works Technical Report*, U.S. Army Corps of Engineers.

Eyring, V., Bony, S., Meehl, G. A., Senior, C. A., Stevens, B., et al. (2016a). “Overview of the Coupled Model Intercomparison Project Phase 6 (CMIP6) experimental design and organization.” *Geoscientific Model Development*, 9(5), 1937–1958.

Eyring, V., Cox, P. M., Flato, G. M., Gleckler, P. J., Abramowitz, G., et al. (2019). “Taking

climate model evaluation to the next level." *Nature Climate Change*, Springer US, 9(2), 102–110.

Eyring, V., Righi, M., Lauer, A., Evaldsson, M., Wenzel, S., et al. (2016b). "ESMValTool (v1.0)-a community diagnostic and performance metrics tool for routine evaluation of Earth system models in CMIP." *Geoscientific Model Development*, 9(5), 1747–1802.

FHWA. (2016a). *Temperature and Precipitation Impacts to Pavements on Expansive Soils: Proposed State Highway 170 in North Texas*. *TEACR Engineering Assessment*, FHWA-HEP-17-018.

FHWA. (2016b). *Temperature and Precipitation Impacts on Cold Region Pavement: State Route 6/State Route 15/State Route 16 in Maine*. *TEACR Engineering Assessment*, FHWA-HEP-17-019.

FHWA. (2017). *Wildfire and Precipitation Impacts to a Culvert: US 34 at Canyon Cove Lane, Colorado*. *TEACR Engineering Assessment*, FHWA-HEP-18-021.

Fischbach, J., Siler-Evans, K., Tierney, D., Wilson, M., Cook, L., et al. (2017). *Robust Stormwater Management in the Pittsburgh Region: A Pilot Study*. RAND Corporation.

Ganguli, P., Kumar, D., and Ganguly, A. R. (2017). "US Power Production at Risk from Water Stress in a Changing Climate." *Scientific Reports*, 7(1), 1–13.

Gelda, R. K., Mukundan, R., Owens, E. M., and Abatzoglou, J. T. (2019). "A Practical Approach to Developing Climate Change Scenarios for Water Quality Models." *Journal of Hydrometeorology*, 20(6), 1197–1211.

Giorgi, F., and Gutowski, W. J. (2015). "Regional Dynamical Downscaling and the Cordex Initiative." *Annual Review of Environment and Resources*, 40(1), 467–490.

Hall, A. (2014). "Projecting regional change." *Science*, 346(6216), 1461–1462.

Hjort, J., Karjalainen, O., Aalto, J., Westermann, S., Romanovsky, V. E., et al. (2018). "Degrading permafrost puts Arctic infrastructure at risk by mid-century." *Nature Communications*, Springer US, 9(1).

Hosseini, M., Tardy, F., and Lee, B. (2018). "Cooling and heating energy performance of a building with a variety of roof designs; the effects of future weather data in a cold climate."

Journal of Building Engineering, Elsevier Ltd, 17(February), 107–114.

Houser, T., Oppenheimer, M., Muir-Wood, R., Rasmussen, D. J., Wilson, P., et al. (2017). "Estimating economic damage from climate change in the United States." *Science*, 356(6345), 1362–1369.

Hyman, R., Kafalenos, R., Beucler, B., and Culp, M. (2014). *Assessment of Key Gaps in the Integration of Climate Change Considerations into Transportation Engineering*. *Transportation Engineering Approaches to Climate Resilience*, FHWA-HEP-15-059.

IPCC. (2017). "Special Reports The Sixth Assessment cycle." <https://www.ipcc.ch/site/assets/uploads/2018/11/AR6_brochure_en.pdf> (Sep. 30, 2019).

Jack, C., and Katragkou, E. (2019). "Evaluation of downscaling methods over Europe: Results of the EU-COST action VALUE." *International Journal of Climatology*, 39(9), 3689–3691.

Jentsch, M. F., James, P. A. B., Bourikas, L., and Bahaj, A. B. S. (2013). "Transforming existing weather data for worldwide locations to enable energy and building performance simulation under future climates." *Renewable Energy*, Elsevier Ltd, 55, 514–524.

Jeong, D. Il, Cannon, A. J., and Zhang, X. (2019). "Projected changes to extreme freezing precipitation and design ice loads over North America based on a large ensemble of Canadian regional climate model simulations." *Natural Hazards and Earth System Sciences*, 19(4), 857–872.

Kermanshah, A., Derrible, S., and Berkelhammer, M. (2017). "Using climate models to estimate urban vulnerability to flash floods." *Journal of Applied Meteorology and Climatology*, 56(9), 2637–2650.

Kilgore, R., Thomas, W. O., Douglass, S., Webb, B., Hayhoe, K., et al. (2019). *Applying Climate Change Information to Hydrologic and Coastal Design of Transportation Infrastructure: Design Practices*. NCHRP Report 15-61.

Kirchhoff, C. J., Barsugli, J. J., Galford, G. L., Karmalkar, A. V., Lombardo, K., et al. (2019). "Climate assessments for local action." *Bulletin of the American Meteorological Society*, 100(11), 2147–2152.

Krakauer, N. Y., and Fekete, B. M. (2014). "Are climate model simulations useful for forecasting

precipitation trends? Hindcast and synthetic-data experiments." *Environmental Research Letters*, 9(2).

Kuo, C. C., Gan, T. Y., and Hanrahan, J. L. (2014). "Precipitation frequency analysis based on regional climate simulations in Central Alberta." *Journal of Hydrology*, Elsevier B.V., 510, 436–446.

Lai, Y., and Dzombak, D. A. (2019). "Use of Historical Data to Assess Regional Climate Change." *Journal of Climate*, 32(14), 4299–4320.

Lai, Y., and Dzombak, D. A. (2020). "Use of the Autoregressive Integrated Moving Average (ARIMA) Model to Forecast Near-term Regional Temperature and Precipitation." *Weather and Forecasting*, 35(3), 959–976.

Lai, Y., and Dzombak, D. A. (2021). "Use of integrated global climate model simulations and statistical time series forecasting to project regional temperature and precipitation." *Journal of Applied Meteorology and Climatology*, 60(5), 695–710.

Mallick, R. B., Radzicki, M. J., Daniel, J. S., and Jacobs, J. M. (2014). "Use of system dynamics to understand long-term impact of climate change on pavement performance and maintenance cost." *Transportation Research Record*, 2455, 1–9.

Mannshardt-Shamseldin, E. C., Smith, R. L., Sain, S. R., Mearns, L. O., and Cooley, D. (2012). "Downscaling extremes: A comparison of extreme value distributions in point-source and gridded precipitation data." *Annals of Applied Statistics*, 6(1), 484–502.

Maraun, D. (2016). "Bias Correcting Climate Change Simulations - a Critical Review." *Current Climate Change Reports*, 2(4), 211–220.

Maraun, D., Brienen, S., Rust, H. W., Sauter, T., Themeßl, M., et al. (2010). "Precipitation downscaling under climate change: Recent developments to bridge the gap between dynamical models and the end user." *Reviews of Geophysics*, 48(3), 1–34.

Maraun, D., Shepherd, T. G., Widmann, M., Zappa, G., Walton, D., et al. (2017). "Towards process-informed bias correction of climate change simulations." *Nature Climate Change*, 7(11), 764–773.

Maraun, D., Widmann, M., and Gutiérrez, J. M. (2018). "Statistical downscaling skill under

present climate conditions: A synthesis of the VALUE perfect predictor experiment." *International Journal of Climatology*, (September), 1–12.

Martel, J.-L., Brissette, F. P., Lucas-Picher, P., Troin, M., and Arsenault, R. (2021). "Climate Change and Rainfall Intensity–Duration–Frequency Curves: Overview of Science and Guidelines for Adaptation." *Journal of Hydrologic Engineering*, 26(10), 03121001.

Meagher, W., Daniel, J., Jacobs, J., and Linder, E. (2012). "Method for evaluating implications of climate change for design and performance of flexible pavements." *Transportation Research Record*, (2305), 111–120.

Mearns, L. O., Gutowski, W. J., Jones, R., Leung, L.-Y., McGinnis, S., et al. (2009). "A regional climate change assessment program." *Eos*, 90(36), 311–312.

Mearns, L. O., McGinnis, S., Korytina, D., Arritt, R., Biner, S., et al. (2017). "The NA-CORDEX dataset, version 1.0." *NCAR Climate Data Gateway. Boulder (CO): The North American CORDEX Program*, 10, D6SJ1JCH.

Melvin, A. M., Larsen, P., Boehlert, B., Neumann, J. E., Chinowsky, P., et al. (2017). "Climate change damages to Alaska public infrastructure and the economics of proactive adaptation." *Proceedings of the National Academy of Sciences*, National Acad Sciences, 114(2), E122–E131.

Merschman, E., Salman, A. M., Bastidas-Arteaga, E., and Li, Y. (2020). "Assessment of the effectiveness of wood pole repair using FRP considering the impact of climate change on decay and hurricane risk." *Advances in Climate Change Research*, Elsevier Ltd, 11(4), 332–348.

Moglen, G. E., and Rios Vidal, G. E. (2014). "Climate change and storm water infrastructure in the mid-atlantic region: Design mismatch coming?" *Journal of Hydrologic Engineering*, 19(11), 1–6.

Moss, R. H., Avery, S., Baja, K., Burkett, M., Chischilly, A. M., et al. (2019). "Evaluating knowledge to support climate action: A framework for sustained assessment. Report of an independent advisory committee on applied climate assessment." *Weather, Climate, and Society*, 11(3), 465–487.

Moss, R. H., Edmonds, J. A., Hibbard, K. A., Manning, M. R., Rose, S. K., et al. (2010). "The

next generation of scenarios for climate change research and assessment." *Nature*, Nature Publishing Group, 463(7282), 747–756.

Musselman, K. N., Lehner, F., Ikeda, K., Clark, M. P., Prein, A. F., et al. (2018). "Projected increases and shifts in rain-on-snow flood risk over western North America." *Nature Climate Change*, Springer US, 8(9), 808–812.

NASEM. (2018). *Review of the New York City Department of Environmental Protection Operations Support Tool for Water Supply*. The National Academies Press, Washington, DC.

Nguyen, M. N., Wang, X., and Leicester, R. H. (2013). "An assessment of climate change effects on atmospheric corrosion rates of steel structures." *Corrosion Engineering Science and Technology*, 48(5), 359–369.

NOAA. (2017). "NOAA Atlas 14 Point Precipitation Frequency Estimates." *Precipitation Frequency Data Server (PFDS)*, <https://hdsc.nws.noaa.gov/hdsc/pfds/pfds_map_cont.html> (Nov. 27, 2018).

O'Neill, B. C., Kriegler, E., Ebi, K. L., Kemp-Benedict, E., Riahi, K., et al. (2017). "The roads ahead: Narratives for shared socioeconomic pathways describing world futures in the 21st century." *Global Environmental Change*, Elsevier Ltd, 42, 169–180.

Palin, E. J., Thornton, H. E., Mathison, C. T., McCarthy, R. E., Clark, R. T., et al. (2013). "Future projections of temperature-related climate change impacts on the railway network of Great Britain." *Climatic Change*, 120(1–2), 71–93.

Peres, D. J., and Cancelliere, A. (2018). "Modeling impacts of climate change on return period of landslide triggering." *Journal of Hydrology*, Elsevier, 567(October), 420–434.

Pierce, D. W., Cayan, D. R., and Thrasher, B. L. (2014). "Statistical Downscaling Using Localized Constructed Analogs (LOCA)." *Journal of Hydrometeorology*, 15(6), 2558–2585.

Rasmussen, D. J., Meinshausen, M., and Kopp, R. E. (2016). "Probability-Weighted Ensembles of U.S. County-Level Climate Projections for Climate Risk Analysis." *Journal of Applied Meteorology and Climatology*, 55(10), 2301–2322.

Reyna, J. L., and Chester, M. V. (2017). "Energy efficiency to reduce residential electricity and

natural gas use under climate change." *Nature Communications*, 8, 1–12.

Robinson, B., and Herman, J. D. (2019). "A framework for testing dynamic classification of vulnerable scenarios in ensemble water supply projections." *Climatic Change*, Springer, 152(3–4), 431–448.

Rosenberg, E. A., Keys, P. W., Booth, D. B., Hartley, D., Burkey, J., et al. (2010). "Precipitation extremes and the impacts of climate change on stormwater infrastructure in Washington State." *Climatic Change*, 102(1–2), 319–349.

Sathaye, J. A., Dale, L. L., Larsen, P. H., Fitts, G. A., Koy, K., et al. (2013). "Estimating impacts of warming temperatures on California's electricity system." *Global Environmental Change*, 23(2), 499–511.

Shen, P. (2017). "Impacts of climate change on U.S. building energy use by using downscaled hourly future weather data." *Energy and Buildings*, Elsevier B.V., 134, 61–70.

Shrestha, S., Bach, T. V., and Pandey, V. P. (2016). "Climate change impacts on groundwater resources in Mekong Delta under representative concentration pathways (RCPs) scenarios." *Environmental Science and Policy*, Elsevier Ltd, 61, 1–13.

Sinha, E., Michalak, A. M., and Balaji, V. (2017). "Eutrophication will increase during the 21st century as a result of precipitation changes." *Science*, 357(6349), 1–5.

Switzman, H., Razavi, T., Traore, S., Coulibaly, P., Burn, D. H., et al. (2017). "Variability of future extreme rainfall statistics: Comparison of multiple IDF projections." *Journal of Hydrologic Engineering*, 22(10), 1–20.

Talukdar, S., and Banthia, N. (2016). "Carbonation in Concrete Infrastructure in the Context of Global Climate Change: Model Refinement and Representative Concentration Pathway Scenario Evaluation." *Journal of Materials in Civil Engineering*, 28(4), 04015178.

Taylor, K. E., Stouffer, R. J., and Meehl, G. A. (2012). "An overview of CMIP5 and the experiment design." *Bulletin of the American Meteorological Society*, 93(4), 485–498.

Terando, A., Reidmiller, D., Hostetler, S. W., Littell, J. S., Beard, Jr., T. D., et al. (2020). "Using information from global climate models to inform policymaking – The role of the U.S. Geological Survey." *Open-File Report 2020–1058*, U.S. Geological Survey, 25.

TRB Superpave Committee. (2005). *Superior Performing Asphalt Pavement SUPERPAVE Performance by Design*. National Academy of Sciences.

Tryhorn, L., and Degaetano, A. (2011). "A comparison of techniques for downscaling extreme precipitation over the Northeastern United States." *International Journal of Climatology*, 31(13), 1975–1989.

Underwood, B. S., Guido, Z., Gudipudi, P., and Feinberg, Y. (2017). "Increased costs to US pavement infrastructure from future temperature rise." *Nature Climate Change*, 7(10), 704–707.

USDOE. (2019). "Coordinated Model Evaluation Capabilities." <https://cmec.llnl.gov/index.html> (Oct. 8, 2019).

Van Vliet, M. T. H., Wiberg, D., Leduc, S., and Riahi, K. (2016). "Power-generation system vulnerability and adaptation to changes in climate and water resources." *Nature Climate Change*, 6(4), 375–380.

Vogel, J., Smith, J., O'Grady, M., Fleming, P., Heyn, K., et al. (2015). *Actionable Science in Practice: Co-producing Climate Change INformation for Water Utility Vulnerability Assessments*. Water Utility Climate Alliance.

Wilks, D. S., and Wilby, R. L. (1999). "The weather generation game: a review of stochastic weather models." *Progress in Physical Geography*, 23(3), 329–357.

Wright, L., Chinowsky, P., Strzepek, K., Jones, R., Streeter, R., et al. (2012). "Estimated effects of climate change on flood vulnerability of U.S. bridges." *Mitigation and Adaptation Strategies for Global Change*, 17(8), 939–955.

Zahmatkesh, Z., Karamouz, M., Goharian, E., and Burian, S. J. (2015). "Analysis of the effects of climate change on urban storm water runoff using statistically downscaled precipitation data and a change factor approach." *Journal of Hydrologic Engineering*, 20(7), 1–11.

Zhang, Y., and Ayyub, B. M. (2018). "Urban Heat Projections in a Changing Climate: Washington, DC, Case Study." *ASCE-ASME Journal of Risk and Uncertainty in Engineering Systems, Part A: Civil Engineering*, 4(4), 1–12.